Int J Comput Vis (2008) 79: 31–43
DOI 10.1007/s11263-007-0088-2

From Inpainting to Active Contours

François Lauze · Mads Nielsen

Received: 17 February 2007 / Accepted: 11 September 2007 / Published online: 17 November 2007

Abstract Background subtraction is an elementary method for detection of foreground objects and their segmentations. Obviously it requires an observation image as well as a background one. In this work we attempt to remove the last requirement by reconstructing the background from the observation image and a guess on the location of the object to be segmented via variational inpainting method. A numerical evaluation of this reconstruction provides a "disocclusion measure" and the correct foreground segmentation region is expected to maximize this measure. This formulation is in fact an optimal control problem, where controls are shapes/regions and states are the corresponding inpaintings. Optimization of the disocclusion measure leads formally to a coupled contour evolution equation, an inpainting equation (the state equation) as well as a linear PDE depending on the inpainting (the adjoint state equation). The contour evolution is implemented in the framework of level sets. Finally, the proposed method is validated on various examples. We focus among others in the segmentation of calcified plaques observed in radiographs from human lumbar aortic regions.

Keywords Segmentation · Inpainting · Active contours · Disocclusion · Adjoint methods · Variational methods

F. Lauze (✉) · M. Nielsen
Nordic Bioscience A/S, Herlev Hovedgade 207, 2370 Herlev, Denmark
e-mail: francois@nordicbioscience.com

M. Nielsen
DIKU, University of Copenhagen, Universitetsparken 1, 2100 Copenhagen, Denmark
e-mail: madsn@diku.dk

1 Introduction: Some Challenging Problems

The three pictures in Fig. 1 represent first: the flag of the Greenland territory; second: an object added on a smooth background via addition of the intensities, similar to the presence of transparent layers, that we will call "pseudo calcification" in the sequel—a typical case would indeed be the one of an X-ray showing a calcific deposit on some soft tissue; and third, a true aortic calcification from a lateral X-ray, with inverted intensities. Contour based active contour methods can provide a segmentation of the circle, although sensitive to the initialization, region based active contours using statistical parameters of intensity/color distributions for each regions, will fail to isolate the circle in the Greenland's flag from the rest of the image, since the two regions have the same statistics! In the pseudocalcification image the difficulty comes also from hardly visible edge information, and the reality is often much worse than this artificial image, while finding discriminating statistical invariants may also prove very difficult. In the case of the true calcification, the bottom of the calcific deposit is only visible by transparency under a dark anatomical structure (hip).

In an attempt to overcome these problems, we introduce a novel methodology, within the framework of active contours. This belongs to the region based family of active contours, but instead of considering that the image domain is partitioned in two (or several regions), our approach consists in considering the following problem: if the region $\tilde{\Omega}$ containing the object of interest is known, and if we have enough prior information on the type of background, can we reconstruct the occluded background image? If we assume a positive answer to that question, then we ask whether a given region Ω contains an object occluding the background

Fig. 1 Challenging inputs for region based active contours. From *left* to *right*: The Greenland's Flag, a pseudo-calcification and a true, inverted X-ray of a aortic calcification

in the following way: if Ω delimits indeed the area occupied by a foreground object, then there should be sufficiently large difference between the observed image and the reconstructed one *within this region*. This leads naturally to a variational problem: if Ω is a given region of the image plane D, u_0 the observed image, $u(\Omega) = \mathcal{I}(u_0, \Omega)$ the reconstructed background and if we call $J(\Omega)$ this background/foreground difference, we may look for the true region $\tilde{\Omega}$ as an extremum for $J(\Omega)$. The goal of this work is to propose such a measure, first in general terms, and then a specific instantiation based on a relatively simple variational inpainting formulation, which essentially corresponds to the TV inpainting of Chan and Shen (Chan and Shen 2002) and a simple measure for discrepancy between two images, based on pixel value differences. The corresponding optimization problem belongs to the class of *optimal control* problems, where the control space is a space of admissible shapes, in our cases, some admissible open sets of the image plane. Then given such an admissible open set or control Ω, its associated state will be the inpainting-denoising of u_0 inside Ω.

We use the shape derivatives tools developed by Delfour and Zolésio (2001) (see also Aubert et al. 2003) in order to derive optimality conditions. In particular, when computing the Gâteaux derivative of our disocclusion criterion with respect to a shape deformation, we retrieve the *shape adjoint state*. From the (informal) computation of the Gâteaux derivative, we deduce, by gradient descent, a curve evolution equation which is then implemented within the framework of level sets.

The paper is organized as follows. In Sect. 2, we give a short review of active contour algorithms. In Sect. 3, we introduce an "disocclusion quality measure", compute its Gâteaux derivative and deduce our inpainting based active contour algorithm from it. Several experiments are presented in Sect. 5 and we conclude in Sect. 6.

This work extends a previous workshop article (Lauze and Nielsen 2005) and the ideas presented here have also been used in a conference paper (Lauze and de Bruijne 2007).

2 Background

Since the seminal paper of Kass, Witkin and Terzopoulos (Kass et al. 1987), active contours have been used rather extensively in computer vision and medical imaging, for the purpose of detection and segmentation, in order to overcome the locality problem of edge detectors. In their original formulation, they are curves with built in regularity properties and preferences for edges in an image. These properties are enforced via an energy minimization. Given an image $u(x, y)$ defined on a domain D, a edge detector, for instance the gradient magnitude image $|\nabla I|$ and a decreasing function $g : [0, \infty] \to \mathbb{R}$, and a curve $C : [0, 1] \to D$, they define the snake energy

$$E(C) = \int_0^1 (\alpha |C_t|^2 + \beta |C_{tt}|^2)\, dt + \int_0^1 g(|\nabla I(C(t)|))\, dt$$

and snakes are minimizers of E. The first part of this energy, the so-called *internal energy* controls the size and the smoothness of the contour, while the second term, the *external energy*, attracts the snake towards the edges of the object in the image. Although very simple to implement, these snakes suffer among other of initialization problems and necessitates reparameterization. In order to overcome initialization problems several solutions were proposed, including balloon forces (Cohen and Cohen 1993), gradient vector flows (Xu and Prince 1997). Geodesic active contours, proposed independently by Caselles et al. (1995) and Kichenassamy et al. (1995) introduced a parametrization independent formulation based on a energy formulation for a candidate contour Γ

$$J(\Gamma) = \int_\Gamma k^{(b)}\, ds$$

where $k^{(b)}$ is a function that should be small at object boundary and s is the arclength parameterization of Γ. When $k^b \equiv 1$, $J(\Gamma)$ is thus simply the length of Γ and the associ-

ated steepest descent equation is the well known Euclidean shortening flow:

$$\frac{\partial \Gamma}{\partial t} = -dJ(\Gamma) = \kappa \vec{n}$$

where κ is the curvature of Γ and $\vec{n}$ is the exterior normal. The effect of k^b is the replace the usual metric on the image plane by one which is image dependent. The resulting steepest descent equation is

$$\frac{\partial \Gamma}{\partial t} = (k^b \kappa - \nabla k^b \cdot \vec{n})\vec{n}.$$

The first term allows shortening to slow down or stop at edges while the second tends to move the contour orthogonally in the direction of an edge.

All these models deal only with contours, not with the regions they separate. A fundamental landmark in image segmentation is the variational formulation of Mumford and Shah (1989)

$$E(u, C) = \frac{1}{2}\int_D (u - u_0)^2\, dx + \frac{\lambda}{2}\int_{D\setminus C} |\nabla u|^2 + \nu \ell(C).$$

A minimizing pair (u, C) represents a piecewise smooth approximation of the input image u_0 on the image plane D, which may have discontinuities along a boundary C, whose length is denoted by $\ell(C)$. Inspired by this approach, Cohen et al. proposed a region based algorithm in Cohen et al. (1993) and some region based strategies were discussed by Ronfard (1994).

Based on a simplification of the Mumford-Shah segmentation functional, Chan and Vese proposed a region based formulation in Chan and Vese (2001). Roughly speaking the image domain should be decomposed as an open "inner part" Ω_i, an open "outer" part $\Omega_o = D\setminus\bar{\Omega}_i$, where $\bar{\Omega}_i$ is the closure of Ω_i and the boundary $\Gamma = \partial\Omega_i$ and Γ is recovered as a minimizer of the following cost function

$$J(\Gamma, a_i, a_o) = \lambda_1 \int_{\Omega_i} (u_0 - a_i)^2\, dx + \lambda_2 \int_{\Omega_o} (u_0 - a_o)^2\, dx + \alpha \ell(\Gamma) + \mu |\Omega_i| \quad (1)$$

where a_i and a_o are reals λ_1, λ_2, α and μ are fixed positive parameters and $|\Omega_i|$ is the area of Ω_i. A trivial computation shows that the optimal a_i and a_o are the average values of u_0 in the inner and outer regions respectively, and a levelset optimization coupled with the estimation of the mean values is performed that attempts to recover two regions such that $|a_i - a_o|$ is as large as possible while enforcing regularity properties for these regions. We will often refer to it as the "Chan-Vese" approach in the sequel.

More complex statistical descriptors have been proposed instead of the mean, as histogram matching in (Aubert et al. 2003). In a series of papers, Paragios and Deriche proposed a paradigm called Geodesic Active Regions where both contour based and region based terms are used (see for instance Paragios and Deriche 2002). General forms for region based energy functionals were studied by Jehan-Besson et al. (2003) with general energy formulation of the form:

$$J(\Omega_i, \Omega_o, \Gamma) = \int_{\Omega_i} k^i(x, \Omega_i)\, dx + \int_{\Omega_o} k^o(x, \Omega_o)\, dx + \int_{\Gamma} k^{(b)}\, ds.$$

The algorithms mentioned above either use a parametric formulation of the different densities in regions and boundaries, such as Gaussian, mixture of Gaussian, parametric description for the distributions of responses of some linear filters as in Heiler and Schnörr (2005) or use a supervised approach: distributions are learned from examples. A non parametric and unsupervised approach has been proposed by Kim et al. (2005), and is based on the mutual information between the distribution of intensities and the regions labeling, seen also as a random variable.

A extensive review and discussion of statistical methods for actives contours and discussion can be found in the work of Cremers et al. (2007). Another excellent reference is Osher and Paragios (2003).

We note nevertheless that in region based active contours, the different regions one want to recover form, together with their boundaries, a partition of the image domain, and that the respective contents of these regions are usually assumed to be independent of each others. While this assumption is sufficient in many applications, the images shown in the previous section show that it may fail.

3 Inpainting Based Segmentation

In this section we introduce background disocclusion ideas and a corresponding variational formulation that will lead to an active contour evolution equation for the segmentation task. We start by the well known background subtraction and discuss elementary ways to recover the support of a foreground object from it. Then inpainting is introduced via statistical inference leading to variational formulations and combining it with support recovery from background subtraction we derive the background disocclusion criterion.

3.1 Background Subtraction and Active Region

A standard approach in detection and tracking is background subtraction. Let us assume that a reference background image u_b is known. If u_0 is now an image of the same scene, with an added object, then a way to detect this object is to compute the pixelwise difference $d(x) = u_0(x) - u_b(x)$ or a function $x \mapsto L(u_b(x), u_0(x))$ measuring the discrepancy between $u_b(x)$ and $u_0(x)$ where the map $(c, d) \mapsto L(c, d)$ is tailored to the problem at hand (when comparing reference and input images, one might expect for instance noise and illumination changes, see Ohta 2001 for an example, but this is a situation that we will not consider here). The region Ω where these discrepancies are large enough is expected to correspond to the location of this object. Depending on the task at hand, a simple thresholding may provide the result, or a more elaborated extraction can be proposed, that will be able to group pixels in a more coherent way. Among these, when considering pixelwise difference $u_0 - u_b$, a good candidate might be the algorithm of Chan and Vese described in the previous section in (1). If we assume only white noise contamination for the background and observations, then difference image should have zero mean in the complement of the foreground region. This means in fact that the parameter a_o describing the average intensity value in this outer region in (1) is expected to be 0 and the algorithm will attempt to evolve the contour in order to *maximize* (in absolute value) the parameter a_i attached to the foreground or inner region in (1):

$$|a_i(\Omega)| = \frac{1}{|\Omega|}\left|\int_\Omega (u_0 - u_b)\,dx\right|$$

while imposing regularity on the boundary via a length term and potentially on the region size via the area term.

Following this rationale, we propose, for a given $r > 0$, to maximize the following criterion

$$K(\Omega; u_b, u_0) = \frac{1}{|\Omega|^r}\left|\int_\Omega L(u_b, u_0)\,dx\right| \tag{2}$$

that can be interpreted as a generalized moment of the discrepancy between u_b and u_0. We could add some regularity constraint to K such as a term of the form $-\alpha\ell(\Gamma)$ where $\Gamma = \partial\Omega$ is the boundary of Ω and α a positive weight, we have not included it, since in practice we did not encounter regularity problems. The introduction of the exponent r in the criterion above allows to control the region size and helps improving "concavity" of our functional. The following sketchy situation, illustrated in Fig. 2 shows its role. The background is a constant image, with value arbitrarily set to 0, and two identical foreground regions Ω_1 and Ω_2 are superimposed to it, say that each object is a unit square with intensity 1. The local pixel discrepancy function

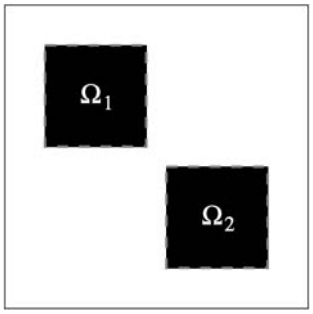

Fig. 2 Role of the area exponent

$L(c, d)$ is chosen as the difference $c - d$. Then for $r = 1$, $K(\Omega_1) = K(\Omega_2) = K(\Omega_1 \cup \Omega_2) = 1$ and in fact any $\Omega \subset \Omega_1 \cup \Omega_2$ is a maximizer for K! In the case $r < 1$ then clearly $K(\Omega_1) = K(\Omega_2) = 1$, while $K(\Omega_1 \cup \Omega_2) = 2^{1-r} > 1$, Ω_1 and Ω_2 are local maximizers for K while $\Omega_1 \cup \Omega_2$ is a global maximizer.

3.2 Background Estimation via Inpainting

Let us now consider the situation where a reference background is not known, but we know instead a distribution for the background images, generally in the form of a distribution of the responses of some local filters over the image sites, say $D = \{s_1, \ldots, s_N\} \subset \mathbb{R}^2$ and $u : D \mapsto \mathbb{R}$,

$$\mathbf{p}(u) = p([f(u, s)]_{s\in D}) = \prod_{s\in D} p(f(u, s))$$

where we have assumed independence of the local filter responses, an assumption used frequently for its computational tractability. In the sequel we assume $f(u, s)$ to be a discrete counterpart of $|\nabla u|$ at location s, for instance

$$f(u, s) = \begin{cases} \sum_{r\in\mathcal{V}(s)} \alpha(|r - s|)|u_r - u_s| & \text{or} \\ \sqrt{\sum_{r\in\mathcal{V}(s)} \alpha(|r - s|)(u_r - u_s)^2} \end{cases}$$

where $\mathcal{V}(s)$ denote the spatial 4- or 8-points neighborhood of pixel location s. For consistency with the continuous setting, α is chosen proportional to $1/|r - s|$ in the first case and $1/|r - s|^2$ is the second. The p.d.f. p is taken as a generalized Laplacian

$$p(x) = \frac{q}{2r\Gamma(1/q)} e^{-|\frac{x}{r}|^q}$$

where $q, r > 0$ and $\Gamma(x)$ is the Euler-Legendre Gamma function.

We now assume that we are given an observed image u_0 from our *unknown* background image u_b with an added object corresponding to an image u_f supported on a subset Ω of D and some white noise η:

$$u_0 = \mathcal{C}(u_b, u_f, \eta)$$

where $\mathcal{C}$ is a combination operation of additive/multiplicative type in the case of a transparent object added on the background, or an XOR-like operation when foreground occludes background, for instance. Our main problem is the determination of Ω, but let us assume we know it. By Bayes's rule of retrodiction, the probability $\mathbf{p}(u|u_0, \Omega)$ of u being the background image knowing u_0 and Ω is given by

$$\mathbf{p}(u|u_0, \Omega) = \frac{\mathbf{p}(u_0|u, \Omega)\mathbf{p}(u|\Omega)}{\mathbf{p}(u_0|\Omega)}. \tag{3}$$

We will assume, for sake of simplicity, that occlusion location is independent of the background, so that $\mathbf{p}(u|\Omega) = \mathbf{p}(u)$ (although in many situations this assumption seems very natural, in one of the situations we have in mind in this article, segmentation of calcifications in radiographs of the lumbar aortic region, the partial occlusion due to the presence of calcification has a tendency to occur along a specific region, the aorta walls, but we won't use it here). We assume that observations are contaminated by Gaussian white noise of variance σ^2. The resulting likelihood term is

$$\mathbf{p}(u_0|u, \Omega) = \prod_{s \in D\setminus\Omega} \frac{1}{\sqrt{2\pi\sigma^2}} e^{\frac{(u_s - u_{0s})^2}{2\sigma^2}}.$$

Then an estimate of the background image can be obtained via a *maximum a posteriori* (MAP) from (3), or, equivalently, neglecting the *evidence* $\mathbf{p}(u_0|\Omega)$ which is constant for a given observed image u_0 and *occlusion locus* Ω, we obtain $\bar{u}$ as a minimizing element for the energy

$$\begin{aligned} E(u; \Omega) &:= E(u; \Omega, u_0) \\ &= -\log \mathbf{p}(u_0|u, \Omega) - \log \mathbf{p}(u) \end{aligned}$$

(we will mostly omit u_0 in E in order to increase legibility). With the previous assumptions on the different probabilities and omitting constants, the MAP estimate becomes, in a continuous setting

$$\begin{aligned} \bar{u} &:= \bar{u}(\Omega) = \operatorname*{argmin}_u E(u, \Omega) \\ &= \int_D \left(\frac{\lambda}{2} \chi_{D\setminus\Omega} (u - u_0)^2 + |\nabla u|^q \right) dx \end{aligned}$$

where $\lambda = r^q/(2\sigma^2)$, D denotes from now an open set of $\mathbb{R}^2$, the image plane, Ω an open included in D and $\chi_{D\setminus\Omega}$ is the characteristic function of $D\setminus\Omega$. For $q = 1$ this is precisely the Total Variation simultaneous inpainting and denoising model of Chan and Shen (2002). In the sequel, we use a slightly modified version of the above inpainting energy

$$E(u; \Omega) = \int_D \left(\frac{\lambda}{2} \chi_{D\setminus\Omega} (u - u_0)^2 + \varphi(|\nabla u|) \right) dx \tag{4}$$

where $\varphi : \mathbb{R} \to \mathbb{R}_+$ is a strictly convex function, increasing for $x > 0$ with $\varphi(x) \approx c|x|^q$ when x becomes large. It is easily seen that q must be at least 1.

With the assumptions we made on q and φ the minimizing element of energy (4) can be shown to exist and be unique in the Sobolev space $W^{1,q}(D)$ when $q > 1$ and in the space of functions of bounded variations $BV(D)$ when $q = 1$ (where there, ∇u replaced by the Radon measure Du, see Aubert and Kornprobst 2006 for details). Boundary conditions (BCs) will be necessary when we have to integrate by part, we choose the very natural zero Neumann ones, i.e. we consider only the functions u that satisfy $\partial u/\partial \vec{n} = 0$ where $\vec{n}$ is the exterior normal to D. In practice, the function φ we used is $\varphi(x) = \frac{1}{q}(\sqrt{x^2 + \epsilon^2})^q$ where ϵ is a strictly positive real number.

A straightforward application of the Calculus of Variations provides the following well known characterization of the minimizer or the inpainting energy: for every function ξ satisfying null Neumann BCs on ∂D and with enough regularity, we set to 0 the directional derivative:

$$\frac{d}{d\tau} E(u + \tau\xi; u_0, \Omega)_{|\tau=0} = 0$$

from which we obtain the variational form for the Euler-Lagrange equation which results from the inpainting energy (4) (we will omit the u_0 in the directional derivative expression in order to alleviate notations)

$$\frac{\partial E(u; \Omega)}{\partial u} = 0$$

where $\frac{\partial E(u;\Omega)}{\partial u}$ is the linear map

$$\begin{aligned} \xi \mapsto \frac{\partial E(u; \Omega)}{\partial u}(\xi) = \int_D \Bigg[& \lambda \chi_{D\setminus\Omega}(u - u_0)\xi \\ & + \frac{\varphi'(|\nabla u|)}{|\nabla u|} \nabla u^T \nabla \xi \Bigg] dx. \end{aligned} \tag{5}$$

An integration by part, using the Neumann BCs on u provides a formal representation of $\frac{\partial E(u;\Omega)}{\partial u}$ and the associated PDE form of the Euler-Lagrange equation

$$\begin{aligned} &\frac{\partial E(u; \Omega)}{\partial u} = 0, \quad \text{where} \\ &\frac{\partial E(u; \Omega)}{\partial u} = \lambda \chi_{D\setminus\Omega}(u - u_0) - \nabla \cdot \left(\frac{\varphi'(|\nabla u|)}{|\nabla u|} \nabla u \right). \end{aligned} \tag{6}$$

3.3 Disocclusion Measure

We finally introduce in this paragraph our variational formulation which will lead to the detection and segmentation algorithm via the formalism of optimal control. As discussed in Sect. 3.1, the knowledge of a background image u_b and

the observation image u_0 allows for defining a numerical criterion measuring the goodness of a candidate detection and we have proposed such a criterion $K(\Omega; u_b, u_0)$ in (2). In the previous paragraph, we argued that, under assumption of the intensity distributions of the background images, the knowledge of the occluding object location Ω allows us to estimate the current background image by minimizing the inpainting energy (4) or solving for the inpainting PDE (6). Combining these ideas, we propose to recover the region $\tilde{\Omega}$ and the disoccluded background estimate $\bar{u}_b$ by solving the constrained problem

$$(\tilde{\Omega}, \bar{u}_b) = \underset{(\Omega, u_b)}{\operatorname{argmax}} \; K(\Omega; u_b, u_0) \tag{7}$$

under the constraint $\frac{\partial E(u_b;\Omega)}{\partial u} = 0$.

The simultaneous estimation of inpainting and segmentation may well seem a hen/egg problem: segmentation via (2) requires the background which in turn can be estimated via inpainting as soon as the segmentation is known. The formulation (7) tackles this apparently paradoxical situation by solving for the segmentation and the inpainting *simultaneously*.

With the assumptions on the inpainting functional made in the previous paragraph, the inpainting energy has a unique solution $u_b(\Omega; u_0)$ for each (admissible) Ω and we can define a numerical criterion that we call *disocclusion measure*

$$\begin{aligned} J(\Omega) &= K(\Omega; \bar{u}(\Omega; u_0), u_0) \\ &= \left| \int_\Omega \frac{L(\bar{u}(\Omega; u_0), u_0)\, dx}{|\Omega|^r} \right|. \end{aligned} \tag{8}$$

It is thus clear that solving the constrained maximization problem (7) defined above is the same as finding a maximizer $\tilde{\Omega}$ of $\Omega \to J(\Omega)$ and the corresponding inpainting $\bar{u}(\tilde{\Omega}; u_0)$.

If a reasonable definition of differentiation with respect to a shape exists, a necessary condition for optimality is to request the shape gradient of J to be null when computed at an optimal shape Ω. In the next section we will propose such an optimization.

4 Optimization via Adjoint Based Method

Given a space of *admissible shapes* $\mathcal{U}^{ad}$, we propose to find an element $\tilde{\Omega} \in \mathcal{U}^{ad}$ which maximizes this disocclusion measure. In order perform the optimization, we will use methods from optimal control theory of systems governed by partial differential equations, their use will transform the optimization problem into a contour evolution equation.

A source of difficulty is the fact that the set of open subsets $\Omega \subset D$ has not the structure of a vector space and differential methods cannot be used directly in order to search for an optimal shape. Instead, we consider variations of Ω according to a flow field $\frac{dx}{dt} = \vec{v}(x, t)$. This will allow us to define the directional derivative $\langle J'(\Omega), \vec{v}(-, 0)\rangle$ at time $t = 0$. This theoretical framework has been used in Computer Vision, especially by Jehan-Besson et al. (2003) as well as Aubert et al. (2003) and recently by Roy et al. (2006).

Adjoint state methods are widely used in control theory, and especially in shape design and control of systems governed by PDEs. We refer the reader to the classical book of J.L. Lions (1971). Some generic presentation can be found in the paper of Ta'asan (1997) or Gunzburger (2001). In the next paragraph we recall some elementary facts from shape analysis and shape differentiation, following Delfour and Zolésio (2001), Aubert et al. (2003) and the actual derivation of optimality conditions for the disocclusion measure will be presented in Sect. 4.2

4.1 Shape Gradients and Shape Derivatives

In the sequel we will assume that Ω is a "sufficiently regular" open set so that we can apply the machinery of shape derivatives as exposed in Delfour and Zolésio (2001). Under the action of a vector field $\vec{v}(x, t) =: \vec{v}$ defined on $\mathbb{R}^2$ for $t \geq 0$, a point $x(t)$ will move through the evolution equation $\dot{x} := \frac{dx}{dt} = \vec{v}(x(t), t)$, from which one defines the transformation $T_t = T_t(\vec{v}) : \mathbb{R}^2 \to \mathbb{R}^2$. When $\vec{v}$ is smooth enough and t sufficiently small, T_t will be a diffeomorphism of $\mathbb{R}^2$ and the image $T_t(\Omega)$ of an open set Ω will be an open set $\Omega(t)$, with $\Omega = \Omega(0)$. Given a function $J(\Omega)$ and $\vec{v}$ one defines the directional derivative of J in the direction of $\vec{v}(\cdot, 0)$ (more simply $\vec{v}$) as the semi-derivative of $\tilde{J}(t) := J(\Omega(t))$ at time 0

$$dJ(\Omega; \vec{v}) := \langle J'(\Omega), \vec{v}\rangle := \lim_{t \to 0+} \frac{J(\Omega(t)) - J(\Omega)}{t}.$$

Under sufficient regularity conditions, that we assume to hold, the map which associates to each vector field $\vec{v}$ the quantity $\langle J'(\Omega), \vec{v}\rangle$ is linear and is called the shape gradient of J at Ω. When $J(\Omega)$ has the integral form

$$\int_\Omega F(x, \Omega)\, dx,$$

it is proved in (Delfour and Zolésio 1989; Delfour and Zolésio 2001) that

$$\langle J'(\Omega), \vec{v}\rangle = \int_\Omega F_s(x, \Omega; \vec{v})\, dx + \int_\Gamma F(x, \Omega)\vec{v} \cdot \vec{n}\, da \tag{9}$$

where $\Gamma = \partial\Omega$ is the (oriented) boundary of Ω, $\vec{n}$ the outward normal to it and a is the arc-length on it and

$$F_s(x,\Omega;\vec{v}) := \left\langle \frac{\partial F}{\partial \Omega}, \vec{v} \right\rangle := \lim_{t\to 0+} \frac{F(x,\Omega(t)) - F(x,\Omega)}{t}$$

is the *shape semi-derivative* or simply *shape derivative* of $F(x,\Omega)$ in the direction of the vector field $\vec{v}$. Standard differentiation rules are valid for shape derivatives and shape gradients.

4.2 The Shape Gradient of the Disocclusion Measure

We now compute the shape gradient for the disocclusion measure (8). Using control terminology, Ω is the *control*, the corresponding inpainting $u(\Omega)$ is the associated *state* and the variational form (5) of the Euler-Lagrange equation associated to the inpainting energy is the *state equation* linking $u(\Omega)$ and Ω.

By shape as well as standard differentiation rules, one obtains

$$\langle J'(\Omega), \vec{v}\rangle = -\frac{r}{|\Omega|^{r+1}}\langle |\Omega|', \vec{v}\rangle \left| \int_\Omega L(u(\Omega),u_0)\,dx \right| \tag{10}$$

$$+ \frac{S}{|\Omega|^r}\int_\Omega L_s(u(\Omega),u_0;\vec{v})\,dx \tag{11}$$

$$+ \frac{S}{|\Omega|^r}\int_\Gamma L(u(\Omega),u_0)\vec{v}\cdot\vec{n}\,da \tag{12}$$

where $S := \operatorname{sign}(\int_\Omega L(u(\Omega),u_0)\,dx)$ comes from the derivative of the absolute value function. The chain rule applies also to the shape derivative of the term (11):

$$L_s(u(\Omega),u_0;\vec{v}) = L_c(u(\Omega),u_0)\left\langle \frac{\partial u(\Omega)}{\partial \Omega}, \vec{v}\right\rangle$$

where L_c is the derivative of $(c,d)\mapsto L(c,d)$ w.r.t. its first variable. The shape gradient of $\Omega \mapsto |\Omega| = \int_\Omega dx$ is given by

$$\langle |\Omega|', \vec{v}\rangle = \int_\Gamma \vec{v}\cdot\vec{n}\,da$$

(when Γ is smooth, this can be directly obtained from Stokes's theorem) and the term (10) is

$$-\frac{rJ(\Omega)}{|\Omega|}\int_\Gamma \vec{v}\cdot\vec{n}\,da.$$

Denoting by $\tilde{u}$ the shape derivative $\langle \frac{\partial u}{\partial \Omega}, \vec{v}\rangle$,

$$\langle J'(\Omega),\vec{v}\rangle = \int_\Gamma \left(-\frac{rJ(\Omega)}{|\Omega|} + \frac{S}{|\Omega|^r}L(u(\Omega),u_0)\right)\vec{v}\cdot\vec{n}\,da + \frac{S}{|\Omega|^r}\int_\Omega L_c(u(\Omega),u_0)\tilde{u}\,dx. \tag{13}$$

The last integral in (13) has to be replaced by an integral on Γ. It includes the shape derivative of the inpainting w.r.t. Ω, which is expressed via the *sensibility equation*, obtained by differentiating the state equation which we recall for the reader's convenience,

$$\begin{aligned}\forall \xi, \quad \xi \mapsto & \frac{\partial E(u;\Omega)}{\partial u}(\xi)\\ &= \int_D \left[\lambda\chi_{D\setminus\Omega}(u-u_0)\xi + \frac{\varphi'(|\nabla u|)}{|\nabla u|}\nabla u^T\nabla\xi\right]dx\\ &= 0.\end{aligned}$$

We get, via the chain rule:

$$\left\langle \frac{d}{d\Omega}\frac{\partial E(u(\Omega),\Omega)}{\partial u}, \vec{v}\right\rangle = \left\langle \frac{\partial^2 E(u(\Omega),\Omega)}{\partial u^2}, \tilde{u}\right\rangle + \left\langle \frac{\partial^2 E(u(\Omega),\Omega)}{\partial\Omega\partial u}, \vec{v}\right\rangle = 0.$$

More precisely, if one defines $\ell(\tau) = \frac{\partial E(u+\tau\tilde{u},\Omega)}{\partial u}$, the sensibility equation asserts that for all ξ with zero Neumann BCs on ∂D,

$$\ell'(0)(\xi) + \left\langle \frac{\partial}{\partial\Omega}\frac{\partial E(u,\Omega)}{\partial u}(\xi), \vec{v}\right\rangle = 0.$$

Note that $\tilde{u}$ must satisfy zero Neumann BCs on ∂D otherwise $u+\tau\tilde{u}$ would not, a fact that we will use below. The quantity $\ell'(0)(\xi)$ is, by a straightforward computation

$$\ell'(0)(\xi) = \int_D \left(\lambda\chi_{D\setminus\Omega}\xi\tilde{u} + \nabla\xi^t A(\nabla u)\nabla\tilde{u}\right)dx, \tag{14}$$

$$A(\nabla u) = \mathcal{H}f(u_x,u_y) \quad f(c,d) = \varphi(\sqrt{c^2+d^2}) \tag{15}$$

where $\mathcal{H}$ denotes the Hessian operator. With the assumptions made on φ in the previous section and the convexity of the Euclidean norm, it follows that $A(\nabla u)$ is (at least formally) positive definite for each $(x,y)\in D$.

On the other hand, a straightforward computation gives

$$\left\langle \frac{\partial}{\partial\Omega}\frac{\partial E(u,\Omega)}{\partial u}(\xi), \vec{v}\right\rangle = -\lambda\int_\Gamma (u-u_0)\xi\,\vec{v}\cdot\vec{n}\,da$$

and we obtain the sensitivity equation

$$\forall\xi, \quad \int_D \left(\lambda\chi_{D\setminus\Omega}\xi\tilde{u} + \nabla\xi^t A(\nabla u)\nabla\tilde{u}\right)dx - \lambda\int_\Gamma (u-u_0)\xi\,\vec{v}\cdot\vec{n}\,da = 0. \tag{16}$$

Add it to (13) to obtain, after re-arranging the terms by boundary integral along Γ and area integral on D,

$$\langle J'(\Omega), \vec{v}\rangle = \int_\Gamma \Big(-\frac{rJ(\Omega)}{|\Omega|} + \frac{S}{|\Omega|^r} L(u(\Omega), u_0) - \lambda(u-u_0)\xi \Big) \vec{v}\cdot\vec{n}\, da + \int_D \Big(\frac{S}{|\Omega|^r} \chi_\Omega L_c(u(\Omega), u_0)\tilde{u} + \lambda \chi_{D\setminus\Omega}\xi\tilde{u} + \nabla\xi^t A(\nabla u)\nabla\tilde{u} \Big) dx. \quad (17)$$

The second integral in the equation above can be rewritten after integration by part in order to eliminate $\nabla\tilde{u}$, using $\tilde{u}$'s zero Neumann BCs, as

$$\int_D \Big(\lambda\chi_{D\setminus\Omega}\xi - \nabla\cdot(A(\nabla u)\nabla\xi) + \frac{S}{|\Omega|^r}\chi_\Omega L_c(u(\Omega), u_0) \Big)\tilde{u}\, dx. \quad (18)$$

Being free to choose ξ, we choose it as solution of the *adjoint state equation*, a linear elliptic equation in ξ

$$\lambda\chi_{D\setminus\Omega}\xi - \nabla\cdot(A(\nabla u)\nabla\xi) = -\frac{S}{|\Omega|^r}\chi_\Omega L_c(u(\Omega), u_0) \quad (19)$$

so that the term (18), or equivalently the second term of (17) *vanishes*. This particular value is called *adjoint state variable* or *costate*. With that choice, the shape gradient becomes

$$\vec{v} \mapsto \langle J'(\Omega), \vec{v}\rangle = \int_\Gamma \Big(-\frac{rJ(\Omega)}{|\Omega|} + \frac{S}{|\Omega|^r} L(u(\Omega), u_0) - \lambda(u-u_0)\xi \Big) \times \vec{v}\cdot\vec{n}\, da.$$

In the following we denote by $\mathcal{F}$ the quantity

$$\mathcal{F} = -\frac{rJ(\Omega)}{|\Omega|} + \frac{S}{|\Omega|^r} L(u(\Omega), u_0) - \lambda(u-u_0)\xi \quad (20)$$

so that $\langle J'(\Omega), \vec{v}\rangle = \int_\Gamma \mathcal{F}\vec{n}\cdot\vec{v}\, da$.

4.3 Curve Evolution, Level Set Formulation and Numerics

Since our goal is to *maximize* the "disocclusion criterion" $J(\Omega)$, we want at each iteration to find the contour evolution $\vec{v}$ that maximizes the gradient of the criterion. The optimal $\vec{v}$ must be, by Cauchy-Schwarz theorem, a positive scalar multiple of $\mathcal{F}\vec{n}$ where $\mathcal{F}$ is defined by (20) and $\vec{n}$ is the outward normal to Γ. The gradient ascent algorithm can be written in a continuous setting as equation $\frac{\partial\Gamma}{\partial t} = \mathcal{F}\vec{n}$. This curve evolution is rewritten into the Osher-Sethian framework of level sets (Sethian 1999) as

$$\psi_t + \mathcal{F}|\nabla\psi| = 0$$

where ψ represents implicitly the evolving contour $\Gamma(t)$ and region $\Omega(t)$ via $\Gamma(t) = \{\psi(\mathbf{x}, t) = 0\}$ and $\Omega(t) = \{\psi(\mathbf{x}, t) < 0\}$. A first order space convex scheme is used to solve this level sets evolution equation, we follow verbatim the numerical techniques discussed by Sethian (1999), Chaps. 5 and 6 (with the obvious adaptation from dimension 3 to dimension 2 in Sethian (1999 , p. 65).

This leads to the following algorithm:

1. Choose an original contour Γ^0, compute ψ^0 as the signed distance function $\psi^0(\mathbf{x}) = \text{dist}_{\Gamma^0}(\mathbf{x})$, and $\Omega^0 = \{\mathbf{x}, H(-\psi^0(\mathbf{x})) = 1\}$, where H is the 1-dimensional Heaviside function
2. For $i = 0$ to $N-1$ or a convergence condition has been fulfilled
   (a) compute the inpainting u^n from the partial differential equation form (6) of the state equation $\frac{\partial E(u^n,\Omega^n)}{\partial u} = 0$,
   (b) compute the adjoint state ξ^n corresponding to (Ω^n, u^n) via (19),
   (c) compute disocclusion measure $J(\Omega^n)$,
   (d) compute $\mathcal{F}^n$ from the previous calculations,
   (e) compute ψ^{n+1} withe the above scheme,
   (f) extract Γ^{n+1} and Ω^{n+1} from it,
   (g) reinitialize ψ^{n+1} as a signed distance $\psi^{n+1}(\mathbf{x}) = \text{dist}_{\Gamma^{n+1}}(\mathbf{x})$
3. Return the optimal pair (Ω^N, u^N).

For stability reasons, the time step Δt is chosen at each iterations as $1/\|\mathcal{F}^n\|_\infty$ (see Sethian 1999, p. 67). The discretization of the divergence term in the inpainting equation $\frac{\partial E(u^n,\Omega^n)}{\partial u} = 0$ follows closely the discretization proposed by Chan and Shen (2002). Using this discretization, we obtain a non linear algebraic system of the form $Q(u) = v$, which we have both solved using a standard fixed point scheme and a linear Gauss-Seidel solver at each fixed point iteration, or as we have also used here, a multigrid solver, implementing a full multigrid (FMG). In this multigrid setting, the downsampling of the discretized characteristic function $\chi_{D\setminus\Omega}$ is performed by a simple nearest neighborhood downsampler, while all the other grid transfer operations use the same operations as in Bruhn et al. (2005). At each level, the error smoother used is a simple non linear Gauss–Seidel with a red-black ordering.

The computation of the adjoint state can be done essentially in two ways: using the discrete adjoint that comes from the numerical gradient of $Q(u)$, a method often used in complex problems, usually associated with automatic differentiators like Odyssée (Rostaing et al. 1993) or ADOL-C (Griewank et al. 1996), or, as we used here, by discretizing directly (19), which is reasonably simple here. It nevertheless requires some care. Indeed, apart from the trivial case, where the matrix A defined in (14) is diagonal, in the case or the quadratic regularizer $\varphi(|\nabla u|) = |\nabla u|^2$, where

$A = Id$, the divergence term will normally contain spatial cross-derivatives and thus needs special attention for the discretization. For that purpose we have used the scheme proposed by Rybak (2004), keeping Chan and Shen discretization for the derivatives of u^n. With this, the linear system resulting from (19) is solved using a Gauss–Seidel solver.

Finally, an important point to mention is that the Heaviside function used is implemented with almost no regularization, as opposed to way it is handled in the level set implementation of most region based algorithms. Too much regularization would bias the inpainting.

5 Experiments

We perform a series of experimentations both on synthetic as well as real data in order to check our approach. A first series is concerned with simple images where contours seem well defined, and because of this simplicity, they allow for an intuitive understanding of the parameters, especially the area weight, and we gradually propose more complex ones. Most of the more complex ones will present (partially) transparent foreground objects over spatially varying backgrounds. We use both some synthetic images as well as real data, X-rays here. We finish with an attempt to use the method with an input that violates largely some of the problem settings.

We have used two choices for the discrepancy function $L(c, d)$. The first choice $L(c, d) = \pm(c - d)$ corresponds to the assumption that the object to be segmented is globally either lighter or darker that the background, and the noise contribution is expected to vanish in the disocclusion criterion: if the observed image u_0 is contaminated by Gaussian white noise $u_0 = \bar{u}_0 + \eta$, $\bar{u}_0$ being an hypothetical noise-free observation, then

$$\begin{aligned}\int_\Omega L(u_b, u_0)\,dx &= \int_\Omega (u_b - u_0)\,dx \\ &= \int_\Omega (u_b - \bar{u}_0)\,dx - \int_\Omega \eta\,dx \\ &= \int_\Omega (u_b - \bar{u}_0)\,dx\end{aligned}$$

since η is white noise.

Because the previous assumption on intensity comparisons between background and foreground is very restrictive, it would for instance not hold for the Greenland's flag example given at the beginning of this paper, we have mostly used the discrepancy function $L(c, d) = |c - d|$.

The inpainting used has normally been the regularized Total Variation one, i.e. $\varphi(s) = \sqrt{s^2 + \varepsilon^2}$ in the energy (4), but quadratic penalizer ($\varphi(s) = s^2$) have also been used.

Figure 3 shows a dark non convex object on a light background with 30% added Gaussian noise. In this experiment, $\lambda = 0.1$, $r = 0.55$. The first row shows a snapshot of the contour evolution at iterations 1, 10, 20 and 30, the second row shows the corresponding domains. We re-did the previous experiment with a more "committed" initialization. It illustrates some stability with respect to the initial contour, as well as the role of the area penalizer exponent r in $|\Omega|^r$ and is illustrated in Fig. 4. We ran two experiments, the first with a value of $r = 0.55$, as in the previous case and the second with a value of $r = 0.60$. In both cases, the λ weight in the data versus inpainting was set to 0.1. In the first case, a correct segmentation has been achieved, while in the sec-

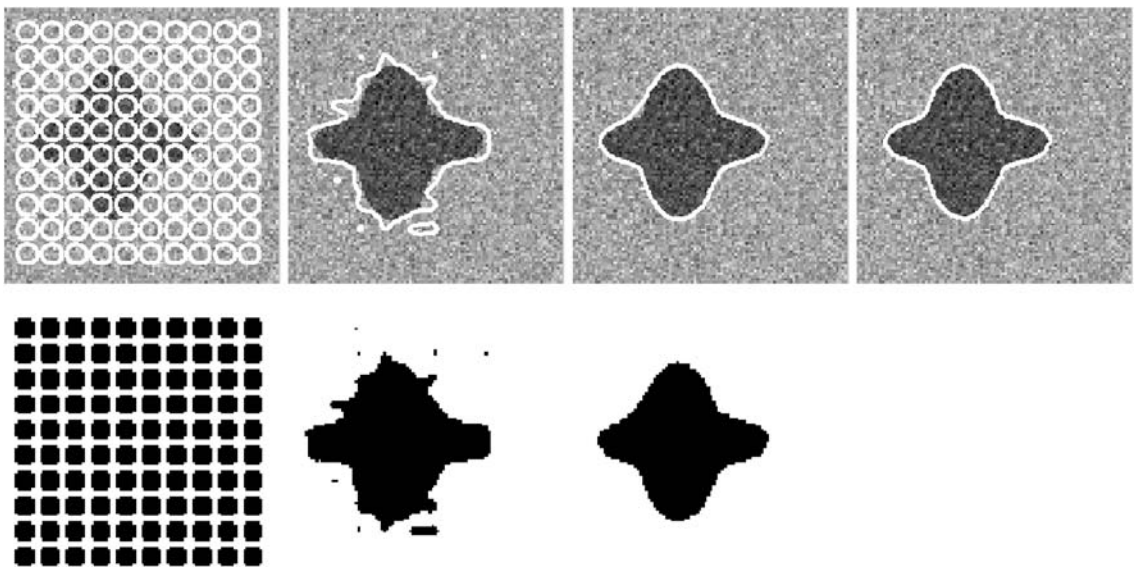

Fig. 3 Segmenting a non convex object, starting from an uncommitted guess

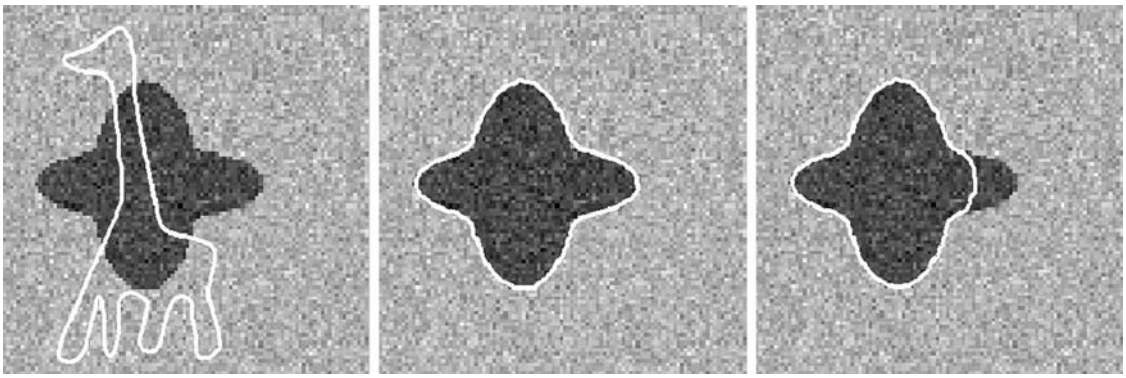

Fig. 4 A more committed starting contour and the effects of the area penalizer. When it is too large, segmentation fails

ond, the right part of the horizontal ellipse could not be fully recovered.

We now show how we overcome some of the limitations of the existing algorithms, first in a simple situation and then in a more complex one. Pictures on Fig. 5 shows how the image was formed: a background with an horizontal linear gradient over which two light squares were added by pixelwise intensity addition, simulating transparency. The combined image is contaminated by Gaussian noise. A human observer perceives the two squares on a changing background, however, by the very construction of such an image, we expect that the algorithm of Chan and Vese finds two "regions", the left and the right parts of the image, separated by a vertical contour which is close of the computed results. Evolutions for the Chan and Vese approach as well as the inpainting based are presented in Fig. 5, showing how in that situation the disocclusion based segmenter is capable of converging to a meaningful result.

A somewhat more complex example, featuring the "pseudo-calcification" image we presented at the beginning of this paper and also in the presence of relatively high Gaussian noise is illustrated here in Fig. 6, another image where Chan-Vese is bound to fail, due to the large variability in the background (a 4th order polynomial). In this example, we used as discrepancy measure the second one: $L(c, d) = |c - d|$, the inpainting was performed with a quadratic penalizer on the gradient.

The next two examples use real calcification images, one of them having been presented in the introduction of this paper. Figure 7 illustrates the behavior of the active contour algorithm on a real X-ray. The segmentation is initialized with a small region which intersection with the calcification is relatively small. The contour will deform and provide finally good quality segmentation.

The next experiment demonstrates the transparency mechanism in action: we segment a calcification which bottom part blends with an anatomical structure—a hip. This is illustrated in Fig. 8. We used as discrepancy measure the absolute value of pixel differences here, with a Total Variation Inpainting denoising.

The last experiment presented here is somewhat an attempt at the impossible. Indeed, using such a simple inpainting method, the algorithm is normally targeted to images with relatively simple content, at least, with a reasonable smoothness assumption. Nevertheless to test the possibilities of our method, we have used a rather complex input image, the third frame from the `Ettlinger-Tor` sequence, frequently used in optical flow estimation. The result presented here are certainly of far lesser quality than some that can be obtained with state of the art algorithms, but show that our method can produce meaningful results, even when the background smoothness assumption is largely violated in this case. The parameters used here where $\lambda = 0.5$ and $r = 2^{-7}$, a very small value. This experiment is illustrated in Fig. 9.

6 Summary and Conclusion

In this paper, we have presented a novel approach for region based active contour segmentation, using the idea of optimal background disocclusion, performed by an inpainting algorithm, which led to a generic variational formulation. Our goal has been to deal with serious non stationarity problems is a series of encountered situation in Computer Vision and Medical Imaging. We showed how two well known ideas, background subtraction and region based active contours could be combined to provide a new type of variational, region based, formulation for segmentation. The resulting algorithm was demonstrated on a series of images.

The computational effort required by this type of computation is relatively heavy, although, thanks to a multigrid solver, can be kept at a reasonable level. It might nevertheless be the price to pay for being able to deal with seemingly complex situations, disocclusion and transparency among others. We have limited to the use of "elementary parts"

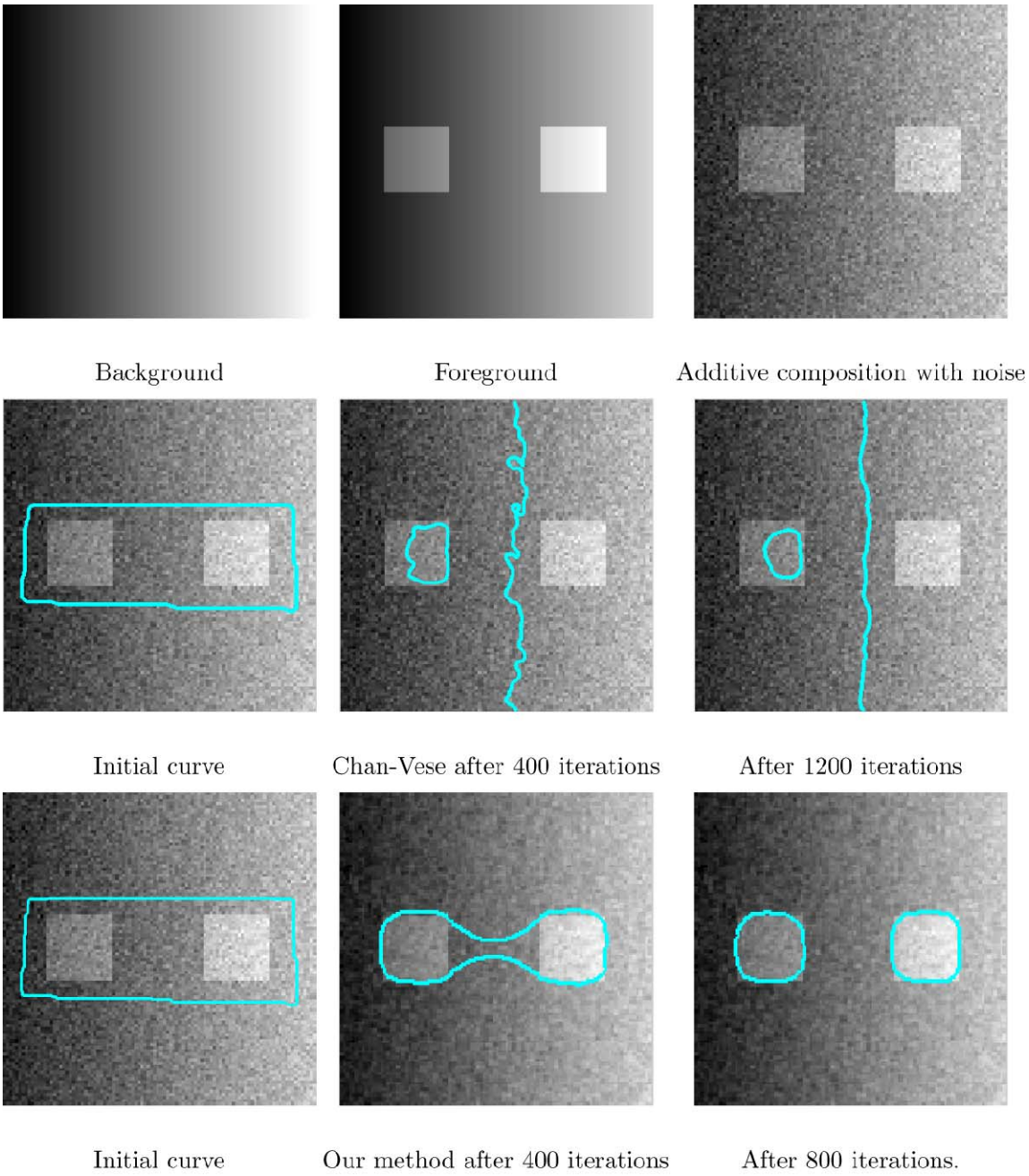

Fig. 5 A linearly varying background with objects added by transparency

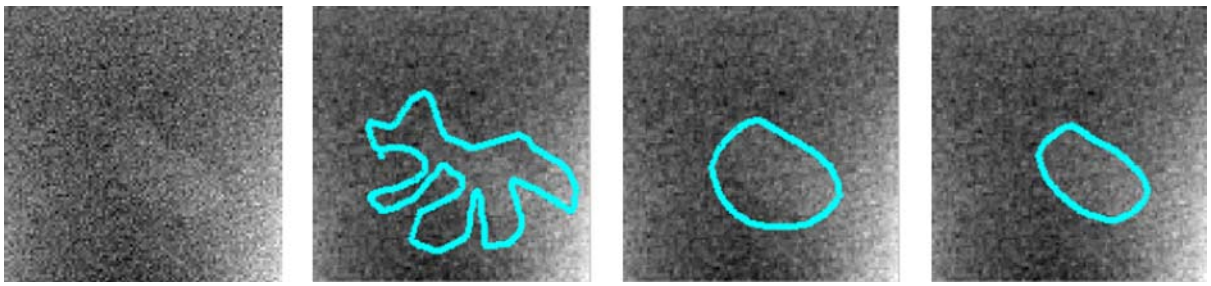

Fig. 6 A noisy synthetic example. From left to right: **a** the pseudo calcification, which has constant gray level value, is added on the spatially varying background with Gaussian white noise of standard deviation 15% of intensity range, **b** the starting contour location, **c** the contour at the middle of evolution and **d** the final contour

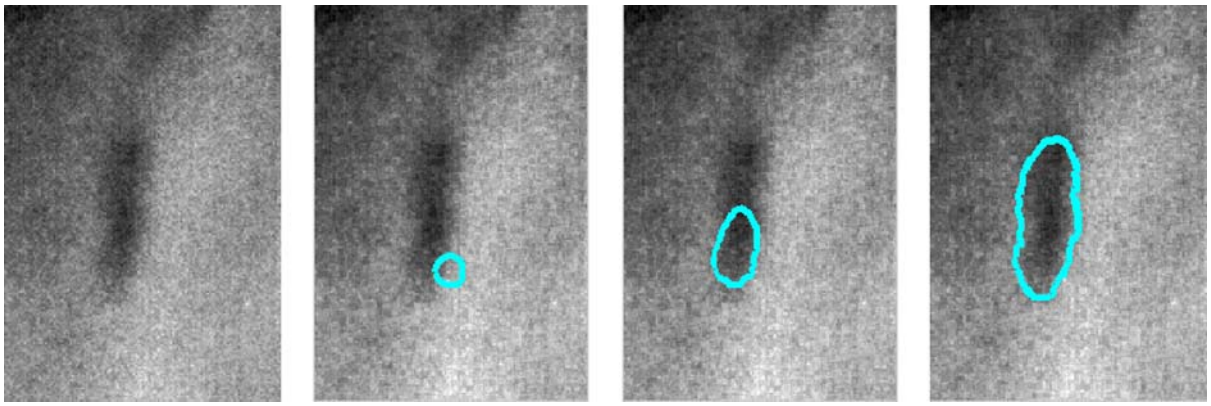

Fig. 7 Evolution of the active contour in a real X-ray. **a** A subimage of the original X-ray (inverted), **b** the starting contour, with only small overlap with the calcific deposit. **c** The contour has "entered" the calcific deposit and start growing, **d** the final segmentation

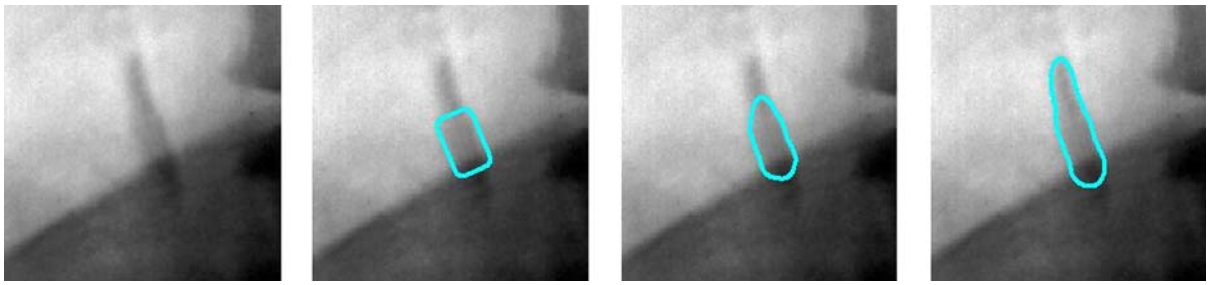

Fig. 8 Evolution of the active contour in a real X-ray: the use of TV inpainting in the background subtraction allows for reconstruction of the hip with in turns provides **a** subimage of the original X-ray (inverted), **b** the starting contour, with only small overlap over the hip. **c** The contour "progresses" on both parts of the hip and **d** the final segmentation

Fig. 9 Can we segment Ettlinger Tor's bus? Using the total variation inpainting. Many difficulties are due to the presence of 1D structures, which are arguably not compatible with the bounded variation assumption on the background image

in constructing our disocclusion measure, we could consider more advanced region based segmentations instead of the Chan-Vese model, as well as more complex inpainting procedures. One could use more sophisticated inpaintings such as Elastica based ones (Ballester et al. 2001; Chan and Shen 2002), but the resulting Euler-Lagrange and Adjoint State equations become much more complex and time consuming to solve.

We are currently working on specializing this approach where either more prior knowledge is available on the objects to be segmented or more on the data is known.

Acknowledgements The `Ettlinger-Tor` sequence is copyright (C) 1998 by H.H. Nagel, KOGS/IAKS Universität Karlsruhe. The calcification images presented here are courtesy of the Center For Clinical and Basic Research (CCBR) A/S, Ballerup, Denmark.

References

Aubert, G., & Kornprobst, P. (2006). *Applied mathematical sciences*: *Vol. 147*, *Mathematical problems in image processing: partial differential equations and the calculus of variations*, 2nd edn. New York: Springer.

Aubert, G., Barlaud, M., Jehan-Besson, S., & Faugeras, O. (2003). Image segmentation using active contours: calculus of variations or shape gradients? *SIAM Journal of Applied Mathematics*, *63*(6), 2128–2154.

Ballester, C., Bertalmio, M., Caselles, V., Sapiro, G., & Verdera, J. (2001). Filling-in by joint interpolation of vector fields and gray

levels. *IEEE Transactions on Image Processing*, *10*(8), 1200–1211.

Bruhn, A., Weickert, J., Feddern, C., Kohlberger, T., & Schnörr, C. (2005). Variational optical flow computation in real time. *IEEE Transactions on Image Processing*, *14*(5), 608–615.

Caselles, V., Kimmel, R., & Sapiro, G. (1995). Geodesic active contours. In *Proceedings of the 5th international conference on computer vision* (pp. 694–699). Boston, MA, June 1995. Los Alamitos: IEEE Computer Society Press.

Chan, T., & Shen, J. (2002). Mathematical models for local nontexture inpainting. *SIAM Journal of Applied Mathematics*, *62*(3), 1019–1043.

Chan, T., & Vese, L. (2001). Active contours without edges. *IEEE Transactions on Image Processing*, *10*(2), 266–277.

Cohen, L. D., & Cohen, I. (1993). Finite-element methods for active contour models and balloons for 2-D and 3-D images. *IEEE Transactions on Pattern Analysis and Machine Intelligence*, *15*(11), 1131–1147.

Cohen, L. D., Bardinet, E., & Ayache, N. (1993). Surface reconstruction using active contour models. In *SPIE conference on geometric methods in computer vision*, San Diego, CA, USA.

Cremers, D., Rousson, M., & Deriche, R. (2007). A review of statistical approaches to level set segmentation: integrating color, texture, motion and shape. *The International Journal of Computer Vision*, *72*(2), April.

Delfour, M. C., & Zolésio, J. P. (1989). Analyse des problèmes de forme par la dérivation des minimax. *Annales de l'Institut Henri Poincaré, Section C*, *S6*, 211–227.

Delfour, M. C., & Zolésio, J.-P. (2001). *Shapes and geometries. Advances in design and control*. Philadelphia: SIAM.

Griewank, A., Juedes, D., & Utke, J. (1996). ADOL–C, a package for the automatic differentiation of algorithms written in C/C++. *ACM Transactions on Mathematical Software*, *22*(2), 131–167.

Gunzburger, M. (2001). Adjoint equation-based methods for control problems in incompressible, viscous flows. *Flow, Turbulence and Combustion*, *65*, 249–272.

Heiler, M., & Schnörr, C. (2005). Natural image statistics for natural image segmentation. *The International Journal of Computer Vision*, *63*(1), 5–19.

Jehan-Besson, S., Barlaud, M., & Aubert, G. (2003). DREAM^{2}S: deformable regions driven by an Eulerian accurate minimization method for image and video segmentation. *The International Journal of Computer Vision*, *53*(1), 45–70.

Kass, M., Witkin, A., & Terzopoulos, D. (1987). Snakes: active contour models. In *First international conference on computer vision* (pp. 259–268), London, June 1987.

Kichenassamy, S., Kumar, A., Olver, P., Tannenbaum, A., & Yezzi, A. (1995). Gradient flows and geometric active contour models. In *Proceedings of the 5th international conference on computer vision* (pp. 810–815). Boston, MA, June 1995. Los Alamitos: IEEE Computer Society Press.

Kim, J., Fisher III, J. W., Yezzi, A., Çetin, M., & Willsky, A. S. (2005). A nonparametric statistical method for image segmentation using information theory and curve evolution. *IEEE Transactions on Image Processing*, *14*(10), 1486–1502.

Lauze, F., & de Bruijne, M. (2007). Toward automated detection and segmentation of aortic calcifications from radiographs. In J. Pluim & J.M. Reinhardt (Eds.), *Medical imaging—SPIE proc-SPIE* (Vol. 6512), SPIE press.

Lauze, F., & Nielsen, M. (2005). From inpainting to active contours. In N. Paragios et al. (Eds.) *LNCS*: *Vol. 3752*. *Proceedings of the third IEEE workshop on variational, geometric and level set methods in computer vision*, Bejing, China, October 2005 (pp. 97–108). New York: Springer.

Lions, J. L. (1971). *Optimal control of systems governed by partial differential equations* (trans: Mitter, S. K.). New York: Springer.

Mumford, D., & Shah, J. (1989). Optimal approximations by piecewise smooth functions and associated variational problems. *Communications on Pure and Applied Mathematics*, *42*, 577–684.

Ohta, N. (2001). A statistical approach to background substraction for surveillance systems. In *International conference on computer vision* (Vol. 2, pp. 481–486). Vancouver, BC, CA, July 2001.

Osher, S., & Paragios, N. (2003). *Geometric level set methods in imaging, vision and graphics*. New York: Springer.

Paragios, N., & Deriche, R. (2002). Geodesic active regions: a new paradigm to deal with frame partition problems in computer vision. *Journal of Visual Communication and Image Representation, Special Issue on Partial Differential Equations in Image Processing, Computer Vision and Computer Graphics*, *13*(1/2), 249–268.

Ronfard, R. (1994). Region based strategies for active contour models. *The International Journal of Computer Vision*, *13*(2), 229–251.

Rostaing, N., Dalmas, S., & Galligo, A. (1993). Automatic differentiation in Odyssée. *Tellus*, *45*(5), 558–568.

Roy, T., Debreuve, E., Barlaud, M., & Aubert, G. (2006). Segmentation of a vector field: dominant parameter and shape optimization. *Journal of Mathematical Imaging and Vision*, *24*(2), 259–276.

Rybak, I. V. (2004). Monotone and conservative difference schemes for elliptic equations with mixed derivatives. *Mathematical Modelling and Analysis*, *9*(2), 169–178.

Sethian, J. A. (1999). *Level set methods and fast marching methods: evolving interfaces in computational geometry, fluid mechanics, computer vision, and materials sciences*. *Cambridge monograph on applied and computational mathematics*. Cambridge: Cambridge University Press.

Ta'asan, S. (1997). *Lecture notes on optimization. 1. Introduction to shape design and control* (Technical report). Von Karman Institue.

Xu, C., & Prince, J. L. (1997). Gradient vector flow: a new external force for snakes. In *International conference on computer vision and pattern recognition* (p. 66).